

Lars Rindorf · Poul Erik Høiby · Jesper Bo Jensen ·
Lars Hagsholm Pedersen · Ole Bang · Oliver Geschke

Towards biochips using microstructured optical fiber sensors

Received: 7 February 2006 / Revised: 7 April 2006 / Accepted: 10 April 2006 / Published online: 8 June 2006
© Springer-Verlag 2006

Abstract In this paper we present the first incorporation of a microstructured optical fiber (MOF) into biochip applications. A 16-mm-long piece of MOF is incorporated into an optic-fluidic coupler chip, which is fabricated in PMMA polymer using a CO₂ laser. The developed chip configuration allows the continuous control of liquid flow through the MOF and simultaneous optical characterization. While integrated in the chip, the MOF is functionalized towards the capture of a specific single-stranded DNA string by immobilizing a sensing layer on the microstructured internal surfaces of the fiber. The sensing layer contains the DNA string complementary to the target DNA sequence and thus operates through the highly selective DNA hybridization process. Optical detection of the captured DNA was carried out using the evanescent-wave-sensing principle. Owing to the small size of the chip, the presented technique allows for analysis of sample volumes down to 300 nL and the fabrication of miniaturized portable devices.

Keywords Microstructured optical fiber · Biosensor · Miniaturization · Lab-on-a-chip · Packaging

L. Rindorf (✉) · J. B. Jensen · O. Bang
COM·DTU,
Department of Communication, Optics and Materials,
Technical University of Denmark,
2800 Kongens Lyngby, Denmark
e-mail: lhr@com.dtu.dk

P. E. Høiby · L. H. Pedersen
Bioneer A/S,
Kogle Allé 2,
2970 Hørsholm, Denmark

O. Geschke
MIC·DTU,
Department of Micro and Nanotechnology,
Technical University of Denmark,
2800 Kongens Lyngby, Denmark

Introduction

Lately there has been a growing interest in using optical fibers for biosensing purposes. This is reflected in a large number of review papers on fiber optic sensors [1–3]. Both solid optical fiber sensors [4–6] and hollow fibers [7–9] have been used for a variety of biochemical detection techniques including fluorescence and absorption measurements. Among numerous recent investigations into applications of fiber optic sensing, selected highlights include the detection of free Cu(II) [10], anthrax [11], protein C [12], the pathogenic bacterium *Listeria monocytogenes* [13], and single nucleotide polymorphism [4]. In a recent journal paper [14], a multi-core MOF was used for the detection of fluorophore-labeled DNA molecules in aqueous solutions.

A solid optical fiber detects reagents on the outside surface, whereas the reagents are positioned inside the air holes in MOF-based biosensors. This poses a problem for the MOF sensor element, since both fluids and probing electromagnetic waves must enter and exit at the end facets of the fiber. If MOFs are to be used as more general sensor components, a robust packaging that allows easy coupling to the surrounding optical and fluidic infrastructure is needed. We have chosen to use a short piece of the same type of MOF applied elsewhere [14] and incorporated it into an optic-fluidic chip for easy handling.

Microstructured optical fibers

Microstructured optical fibers [15, 16] are characterized by having a plurality of air holes running along the entire length of the fiber. The optical properties of this class of fibers are determined by the geometry, size, and relative position of the air holes. By varying these parameters, MOFs with strong evanescent fields in the air holes can be designed and fabricated. The majority of MOFs produced worldwide are based on silica [15, 16], the standard basis material for the fabrication of optical fibers. Recently, there has also been increasing interest in fabricating MOFs in

other materials such as polymers [17] or soft glasses [18]. The fabrication method is usually determined by the fiber material. For silica-based MOFs, the stack-and-draw technique [16] is by far the most used technique. Capillary tubes are stacked and drawn to a pre-form that is heated to approximately 2,000 °C and drawn to a fiber. This method has its limitations with respect to the freedom in the relative position of the air holes given by the stacking of individual silica capillary tubes. The method has still been very successful, and is capable of producing fibers with optical properties that cannot be obtained by using conventional solid optical fibers. For polymer-based fibers, the air hole structure is most commonly defined by drilling holes in a solid pre-form as described elsewhere [17]. Polymer-based MOFs can be drawn directly from such a pre-form at temperatures in the range of a few hundred degrees Celsius depending on the polymer material. One major advantage of MOFs compared to standard solid optical fibers is the possibility of obtaining a strong overlap between light guided through the fiber and samples positioned in the air holes without removing the protective coating and cladding of the fiber. A picture of the silica-based Air-15-1550 MOF [19] used in this paper is shown in Fig. 1. This fiber is 125 μm in diameter with a large center hole 17 μm in diameter surrounded by a periodic structure of 312 smaller holes 2.3 μm in diameter.

Principle

Evanescent wave sensing

The optical sensor presented in this paper relies on the principle of evanescent waves. The electromagnetic field from light propagating through the fiber is mostly confined to the glass, but due to the wave nature of electromagnetic waves an exponential tail of the optical field will penetrate into the holes of the MOF and thereby probe any sample placed there. Therefore, the system acts as a highly advanced capillary tube with strong sample–light interaction. As described above, the microstructured part of the fiber used in our experiments consists of a large number of

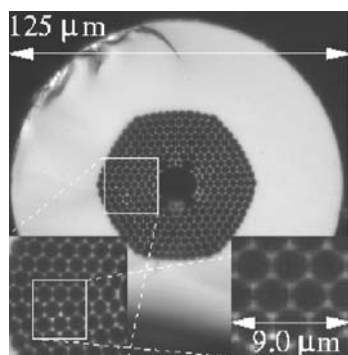


Fig. 1 Cross-section of the MOF integrated in the optic-fluidic chip. The diameter of the microstructured part of the fiber is 65 μm , and the large and small holes are 17 μm and 2.3 μm in diameter, respectively

air holes. Between every three neighboring holes there is a small core-like structure (depicted in the inset of Fig. 1). The fiber can hence be operated as a multi-core waveguide consisting of an ensemble of 564 highly sensitive fiber micro-sensors embedded in the sample. To demonstrate the efficiency of this design, we have calculated the fraction of the optical field intensity that penetrates into the water-filled holes using electromagnetic field simulations [20]. The larger the fraction of the field that propagates as this evanescent wave, the stronger the interaction between the optical field and samples placed in the air holes.

As seen in Fig. 2, this fraction depends on the wavelength of the electromagnetic wave. It is also observed that at a wavelength of 650 nm, 6.5% of the field intensity is in the air holes of the multi-core MOF. In comparison, our calculations show that in a design by Kiiveri et al. [7], the penetration of the optical field into the sample, and hence the sensitivity of the sensor, is 100 times smaller than in the multi-core MOF. Their fiber has a single large air hole 100–300 μm in diameter whose edge has a thin layer of doped silica with higher refractive index (as seen in the insert of Fig. 2). Furthermore, the multi-core MOF has a large surface ($A=37 \text{ mm}^2$) to volume (24 nL) ratio ($A:V$) of $1.5 \times 10^3 \text{ mm}^{-1}$. In comparison, the fiber presented by Kiiveri has an $A:V$ ratio of approximately 20 mm^{-1} . The large surface-to-area ratio in the multi-core MOF ensures a very efficient interrogation of the sample injected into the fiber. By closer inspection of Fig. 1, one might suspect that light coupled into the solid silica that surrounds the microstructure might disturb the optical detection that is based on absorption spectroscopy on Cy3 fluorophores. Fortunately, there is a high propagation loss in this part of the fiber, and this does hence not pose a problem.

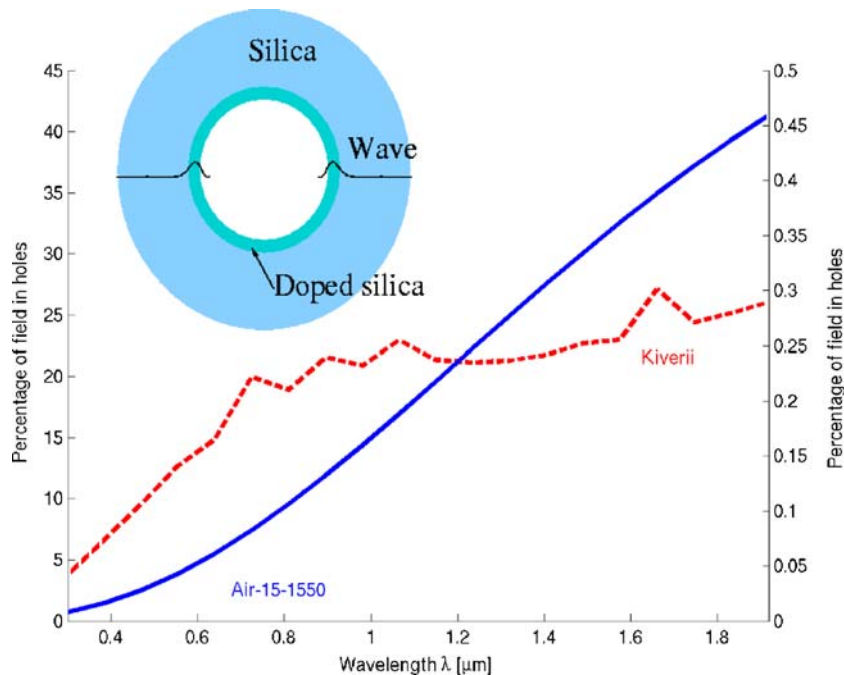
Integration of MOF into an optic/fluidic chip

A 16-mm-long piece of the multi-core MOF is integrated into a CO_2 -laser-machined [21, 22] PMMA chip (Fig. 3). The PMMA is Plexiglas XT, clear 20070, 1.5-mm plates.

The construction of the chip is designed around the MOF. Each end of the MOF is connected to a capillary tube and a large-core conventional multimode fiber (Fig. 4). The microstructured part of the MOF and the core of the multimode fiber are similar in size, 65 μm and 62.5 μm in diameter, respectively. The relatively large diameters of the fibers make the fiber-to-fiber alignment relatively easy compared to working with single-mode fibers with core radii in the order of 5–10 μm . The capillary tube (Upchurch Scientific FS-150) is made of silica and has an inner diameter of 50 μm .

The chip is fabricated in a three-step process. First the grooves for the fibers and capillary tubes are cut in a piece of PMMA using a CO_2 laser. A lid with channels that allows glue to enter the chip is also fabricated in PMMA. Secondly, the lid and bottom pieces are heat bonded in a convection oven for 2 h at 110 °C. Finally, the 16-mm-long piece of MOF is carefully inserted into the chip and glued into place with epoxy resin delivered through the glue

Fig. 2 Percentage of the electromagnetic wave in the water-filled holes as function of wavelength for the multi-core MOF (left y-axis) and a fiber design by Kiveri et al. [7] (right y-axis). The inset shows the facet of the fiber used by Kiveri and co-workers



channels. The glue channels make use of capillary forces to pull the glue into the chip. To avoid the glue from flooding the chip, its design is such that glue channels widen at their ends making the capillary forces stop the further flow of the glue. After inserting the MOF, the large-core multimode fibers and the capillary tubes are inserted. The total inner volume of the chip is 300 nL.

For microfluidic tubes, the flow resistance increases rapidly with decreasing radii as R^{-4} . This means that the flow rate through the small air holes (diameter 2.3 μm) in the multi-core MOF is almost 3,000 times smaller than the flow rate through the large air hole (17- μm diameter). Only 10 nL of the chip's total internal volume of 300 nL is

constituted by the fiber sensor. The rest is dead volume in the fluidic channels outside the fiber. The slow flow rate of the small holes can cause problems with clearing this dead volume, but here the fiber's larger 17 μm hole comes to aid. This larger hole has a flow rate that enables the dead volume of the chip to be cleared of sample liquids in minutes, while without it the time required would be of the order of 1 h.

Experiments

For the optical characterization of the sensor chip probed by various aqueous solutions we used standard absorption spectroscopy. Transmission spectra were recorded using a white-light Halogen light source (Ocean Optics HL-2000 [23]) and a highly sensitive spectrometer (Ocean Optics HR2000). The absorption caused by the Cy3 label



Fig. 3 Fabricated lab-on-a-chip component with integrated MOF. The MOF is optically connected to input/output optical fibers (coming from left and right). Fluid samples are injected into the MOF through silica capillary tubes

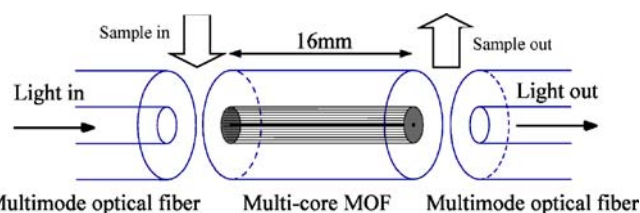


Fig. 4 A MOF with multimode fibers aligned at each end. The cores of the multimode fibers and the microstructured part of the MOF are similar in size. For efficient coupling of light from the “input” fiber to the MOF and further to the “output” fiber, the alignment of the fibers needs to be precise within ± 5 μm . The microstructure of the MOF is shown in Fig. 1. A distance of few tens of micrometers between the coupling fibers and the MOF is sufficient to allow the sample to enter the air holes of the MOF while still limiting the optical coupling loss

molecules attached to the DNA was assessed by comparing with a reference measurement.

Immobilization of sensor layer

The sample under investigation is introduced into the chip through the capillary tubes by inserting one of these into a small vessel containing the liquid sample as shown in Fig. 3. The vessel is then pressurized by connecting it to a pressure chamber. In this manner a pressure difference of 0–5 bar can be maintained over the 16-mm length of MOF so that the liquid sample is pressed through the MOF. In the experiments we perform hybridization between a Cy3-labeled single-stranded oligo-DNA (target DNA) and a complementary single-stranded oligo-DNA (capture DNA) immobilized inside the holes of the MOF. The immobilization procedure is performed with fairly standard techniques involving electrostatic coupling of an anionic long-chained polymer to the negatively charged silica surface. This is followed by a stepwise introduction of chemicals that will bind and make the surface suitable for immobilizing DNA molecules (Fig. 5).

The whole process is performed on the inner surface of the MOF integrated into the chip using the following procedure. First, the chip is filled with poly(L-lysine) (1:1,000 in H₂O, w/v, Sigma) for 3 min by applying a 1-bar pressure difference. This overpressure is then removed, and the chemical is allowed to work for another 7 min with the liquid at rest. The chip is then washed with PBS (10 mM NaH₂PO₄/Na₂HPO₄ pH 7.4, 150 mM NaCl) for 5 min to remove excess poly(L-lysine) that has not been immobilized on the silica surface. Glutaraldehyde (12.5%) which is suitable for connecting two positively charged molecules (in our case poly(L-lysine) and streptavidin) is then introduced for 3 min at 1-bar external pressure and allowed to work for 17 min with the liquid at rest followed by a 5 min PBS wash. This is then followed by the introduction of the biotin-binding protein streptavidin (1 mg mL⁻¹ in PBS) for 3 min at 1-bar overpressure and another 12 min without external pressure. Ethanolamine (40 mM) is used to block the empty sites on the glutaraldehyde not occupied by streptavidin, so that the following sample of biotin-labeled capture DNA does not immobilize itself outside the biotin binding site on streptavidin. This is again

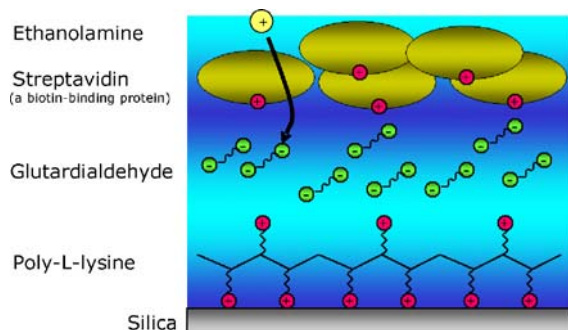


Fig. 5 Schematic drawing of a modified silica surface making it capable of immobilizing DNA molecules

followed by a 5-min wash with PBS. A 10 μ M solution of biotin-labeled single-stranded DNA capture molecules (sequence 5'-biotin-CAGCGAGGTGAAAACGACAAAAGGGG) is then introduced for 3 min at 1 bar and 12 min without external pressure. The capture complex is then complete and the chip is ready for the DNA hybridization experiment.

DNA hybridization

Two sets of experiments are performed using the same chip: a pure reference sample containing the non-complementary Cy3-labeled oligo-DNA (non-target DNA, sequence 5'-Cy3-CTTAGGTCATTCTAAGAATCGATACT) and a pure sample containing the complementary Cy3-labeled oligo-DNA (target DNA, sequence 5'-Cy3-CCCCTT TTGTCGTTTTACCTCGCTG). A reference transmission spectrum of the sensor chip is obtained prior to the injection of the samples.

First a sample (10 μ M) of the non-target DNA is introduced into the capture DNA (Fig. 6, 1a) for 5 min at 1-bar overpressure and allowed to hybridize to the capture DNA for 40 min with the sample at rest. The spectrometer reads a clear absorption signal from the Cy3 fluorescent molecule. The chip is then washed for 20 min with PBS at 1 bar (Fig. 6, 2a). The Cy3 signal rapidly diminishes at the start of the wash. After the wash, the signal from the non-target sample is recorded. The procedure is then repeated with the target DNA (10 μ M) (Fig. 6, 1b–2b). Transmission spectra are recorded after each step (1a, 1b, 2a, and 2b) and by comparing with the reference measurement, the absorption caused by the Cy3 molecules is derived.

Results and discussion

The results of the experiments are presented in Fig. 7.

The results show that DNA has been captured in the chip and that this capture is selective. Initially, when the samples containing the non-complementary (1a) and the complementary (1b) DNA strings are placed in the fiber, the absorbance is high. The difference (approximately 14%) between the two absorption curves is probably due to a hybridization-induced up-concentration of DNA molecules at the surface of the air holes where the optical field intensity is higher than elsewhere in the holes. When the samples are washed out, the signal from the complementary sample (2b) is now 4 times stronger than the signal from the non-complementary (2a) sample indicating a good selectivity of the process. When calculating the absolute absorbance, the inhomogeneous field intensity in the MOF must be taken into account. When using a MOF sensor element, the spectrometer does not record the actual absorbance of the fluorescent molecules. The true absorbance of the molecules can be found by correcting for the actual field intensity at the surface of the air holes that is smaller than the average field intensity and varies with wavelength. The field intensity is calculated using electro-

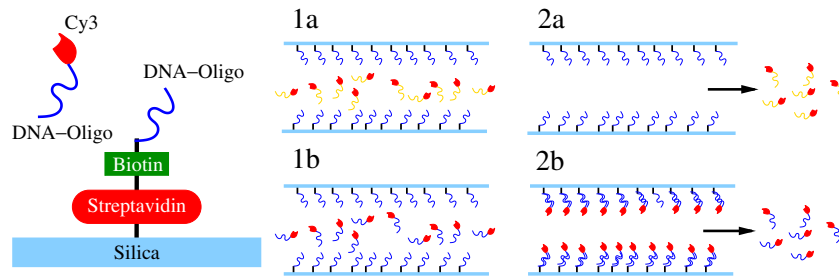


Fig. 6 Principle of DNA capture inside the air holes of the MOF. The silica side walls are coated with a sensing layer containing single-stranded capture DNA oligoes (*far left*). The Cy3-labeled non-target DNA sample is introduced into the fiber (*1a*), allowed to hybridize and subsequently washed (*2a*) for the removing of unbound DNA. In this case no hybridization occurs and the non-

target DNA is washed out. Then the same procedure is performed with a sample of Cy3-labeled target-DNA (*1b, 2b*), and in this case hybridization takes place, and only excess target DNA is washed out. The hybridization efficiency and thus the presence of target- and non-target DNA can be detected via the fluorescent Cy3 molecule

magnetic field simulation [20]. The corrected absorbance spectrum is displayed in Fig. 7. With the corrected absorbance Lambert–Beers law ($A=\epsilon cl$) can be used to estimate the amount of sample present in the 24-nL volume of the MOF. Using the value $\epsilon=1.5\times 10^5\text{ cm}^{-1}$ at $\lambda=546\text{ nm}$ we estimate the amount of sample to be approximately 200 pmol.

The signal observed from the mismatch sample is believed to be caused by a combination of clogging of the MOF holes and non-specific binding to the surface, which is a common phenomenon within DNA hybridization. The non-specific binding can be reduced by increasing the stringency (harshness) of the wash, but this will also result in reduced hybridization efficiency between the capture DNA and the target DNA. Furthermore, temperature control can be integrated on the chip to increase the stringency of the hybridization process. The clogging can be reduced by filtering the sample.

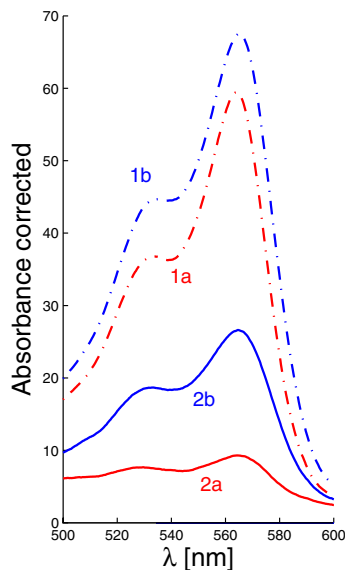


Fig. 7 Absorbance after the injection of the non-complementary (*1a, 2a*) and complementary (*1b, 2b*) DNA. Absorbance is recorded when the sample is in the fiber (*1a, 1b*), and after washing (*2a, 2b*). Absorbance is corrected for the inhomogeneous field intensity in the MOF

When comparing our PCF chip-based detection technique with other optical-fiber-based detection methods it is evident that the PCF-based device has two major advantages. One is the robustness of the fiber sensor element itself. When using conventional solid optical fibers for evanescent wave sensing, the protective fiber coating and cladding needs to be removed to ensure an overlap between the optical field and the sample it probes. Thereby the fiber becomes very fragile. In a PCF, the air holes allow the sample to be brought into contact with the fiber core. There is hence no need to remove the coating and the fiber remains robust while still being able to function as an evanescent wave sensor. Secondly, capillary tubes such as the one presented in the inset of Fig. 2 are robust, but have as poor surface-to-volume ratio compared to the PCF used in the present paper. The PCF-based sensor hence utilizes the available sample volume much more efficiently.

One of the major tasks in the future improvements of the chip described in this paper concerns the alignment of the MOF and the multimode fibers. This can be a challenging task, especially because a tight seal around the MOF multimode fibers is needed to reduce the dead volume and memory effects. Other techniques for integrating the MOF-based sensor element in an optic-fluidic component are currently being investigated.

One of the potential applications of the integrated MOF-based sensor element is real-time monitoring of the selective capture processes involving for instance DNA hybridization or antigen–antibody binding events. We are currently doing several investigations in this field.

Another aspect that might facilitate the experimental handling is to use polymer microstructured optical fibers. The surface chemistry of many polymers makes them much more suitable for coating, and thus makes the process of immobilizing molecules [24] easier compared to silica.

Conclusions

The results presented here show that microstructured optical fiber (MOF)-based sensor elements can be integrated into a lab-on-a-chip component. The lab-on-a-chip presented is successfully used in a selective DNA

capture experiment. The design of the lab-on-a-chip allows for continuous control of liquid flow through the MOF and simultaneous optical characterization. The sample volume is only 10 nL, and the total internal volume is 300 nL. Our lab-on-a-chip design allows for the integration of MOFs along with other existing lab-on-a-chip components, and this should open new possibilities for lab-on-a-chip technology.

Acknowledgements We would like to thank the Danish ministry of Science, Technology, and Innovation (VTU, Centre Contract μ KAP) and the Technical University of Denmark for their financial support. Crystal-Fibre A/S is acknowledged for providing the multi-core microstructured optical fiber [19].

References

1. Wolfbeis OS (2004) *Fresenius J Anal Chem* 76:3269–3283
2. Monk DJ, Walt DR (2004) *Anal Bioanal Chem* 379:931–945
3. Brogan KL, Walt DR (2005) *Curr Opin Chem Biol* 9:494–500
4. Watterson JH, Raha S, Kotoris CC, Wust CC, Gharabaghi F, Jantzi SC, Haynes NK, Gendron NH, Krull UJ, Mackenzie AE, Piunno PAE (2004) *Nucleic Acids Res* 32:Art No e18
5. Zhang J, Dong JH, Luo M et al (2005) *Langmuir* 21:8609–8612
6. Zhang J, Luo M, Xiao H et al (2006) *Chem Mater* 18:4–6
7. Kiiveri P, Hokkanen A, Kylmänen R, Keinänen K, Tammela S (1996) *Proc of SPIE* 2695:169–179
8. Dhadwal HS, Kemp P, Aller J et al (2004) *Anal Chim Acta* 501:205–217
9. Lippitsch ME, Draxler S, Kieslinger D, Lehmann H, Weigl BH (1996) *Applied Optics* 35(19):3426–3431
10. Zeng H-H, Thompson RB, Maliwal BP, Fones GR, Moffett JW, Fierke CJ (2003) *Anal Chem* 75:6807–6812
11. Tims TB, Lim DV (2004) *J Microbiol Methods* 59:127–130
12. Tang L, Kwon HJ, Kang KA (2004) *Biotechnol Bioeng* 30:869–879
13. Geng T, Morgan MT, Bhunia AK (2004) *Appl Environ Microbiol* 70:6138–6146
14. Jensen JB, Pedersen LH, Hoiby PE, Nielsen LB, Hansen TP, Folkenberg JR, Riishede J, Noordegraaf D, Nielsen K, Carlsen A, Bjarklev A. (2004) *Optics Lett* 29:1974–1976
15. Russell PStJ (2003) *Science* 299: 358–362
16. Knight JC, Birks TA, Russell PStJ, Atkin DM (1996) *Optics Lett* 21:1547–1549
17. Eijkelenborg MA v., Large MCJ, Argyros A, Zagari J, Manos S, Issa NA, Bassett I, Fleming S, McPhedran RC, de Sterke CM de, Nicorovici APN (2001) *Optics Express* 9:319–327
18. Feng X, Monro TM, Petropoulos P, Finazzi V, Richardson DJ (2005) *Appl Phys Lett* 87:081110
19. Crystal Fibre A/S homepage: <http://www.crystal-fibre.com>
20. MIT Photonic Bands software, <http://ab-initio.mit.edu/mpb>
21. Klank H, Kutter JP, Geschke O (2002) *Lab-on-a-chip* 2: 242–246
22. Geschke O, Klank H, Telleman P (2004) *Microsystem engineering of lab-on-a-chip devices*. Wiley-VCH, Weinheim
23. Ocean Optics homepage: <http://www.oceanoptics.com/>
24. Jensen JB, Hoiby PE, Emiliyanov G, Bang O, Pedersen LH, Bjarklev A (2005) *Optics Express* 15:5883